

Fabrication of Acidic pH-Cleavable Polymer for Anti-Cancer Drug Delivery Using a Dual Functional Monomer

Luping Zheng, Xiaolong Zhang, Yunfei Wang, Fangjun Liu, Jinlei Peng, xuezhi zhao, Huiru Yang, Liwei Ma, Baoyang Wang, Cong Chang, and Hua Wei

Biomacromolecules, **Just Accepted Manuscript** • DOI: 10.1021/acs.biomac.8b01001 • Publication Date (Web): 14 Aug 2018

Downloaded from <http://pubs.acs.org> on August 14, 2018

Just Accepted

“Just Accepted” manuscripts have been peer-reviewed and accepted for publication. They are posted online prior to technical editing, formatting for publication and author proofing. The American Chemical Society provides “Just Accepted” as a service to the research community to expedite the dissemination of scientific material as soon as possible after acceptance. “Just Accepted” manuscripts appear in full in PDF format accompanied by an HTML abstract. “Just Accepted” manuscripts have been fully peer reviewed, but should not be considered the official version of record. They are citable by the Digital Object Identifier (DOI®). “Just Accepted” is an optional service offered to authors. Therefore, the “Just Accepted” Web site may not include all articles that will be published in the journal. After a manuscript is technically edited and formatted, it will be removed from the “Just Accepted” Web site and published as an ASAP article. Note that technical editing may introduce minor changes to the manuscript text and/or graphics which could affect content, and all legal disclaimers and ethical guidelines that apply to the journal pertain. ACS cannot be held responsible for errors or consequences arising from the use of information contained in these “Just Accepted” manuscripts.



1
2
3
4
5
6
7
8
9
10
11
12
13
14
15
16
17
18
19
20
21
22
23
24
25
26
27
28
29
30
31
32
33
34
35
36
37
38
39
40
41
42
43
44
45
46
47
48
49
50
51
52
53
54
55
56
57
58
59
60

Fabrication of Acidic pH-Cleavable Polymer for Anticancer Drug Delivery Using a Dual Functional Monomer

Luping Zheng,^{†,#} Xiaolong Zhang,^{†,#} Yunfei Wang,[†] Fangjun Liu,[†] Jinlei Peng,[†] Xuezhi Zhao,[†]
Huiru Yang,[†] Liwei Ma,[†] Baoyan Wang,[†] Cong Chang^{*,‡}, and Hua Wei^{*,†}

[†] State Key Laboratory of Applied Organic Chemistry, Key Laboratory of Nonferrous Metal Chemistry and Resources Utilization of Gansu Province, and College of Chemistry and Chemical Engineering, Lanzhou University, Lanzhou, Gansu 730000, China

[‡] Department of Pharmaceutics, School of Pharmacy, Hubei University of Chinese Medicine, Wuhan, Hubei 430065, China

[#] These authors contributed equally to this paper.

*Corresponding authors

E-mail addresses: weih@lzu.edu.cn (H. Wei) or 1126@hbtcn.edu.cn (C. Chang)

Abstract: The preparation of tumor acidic pH-cleavable polymers generally requires tedious post-polymerization modifications, leading to batch-to-batch variation and scale-up complexity. To develop a facile and universal strategy, we reported in this study design and successful synthesis of a dual functional monomer, *a*-OEGMA that bridges a methacrylate structure and oligo(ethylene glycol) (OEG) units via an acidic pH-cleavable acetal link. Therefore *a*-OEGMA integrates (i) the merits of commercially available oligo(ethylene glycol) monomethyl ether methacrylate (OEGMA) monomer, *i.e.*, hydrophilicity for extracellular stabilization of particulates and a polymerizable methacrylate for adopting controlled living radical polymerization (CLRP), and (ii) an acidic pH-cleavable acetal link for efficiently intracellular destabilization of polymeric carries. To demonstrate the advantages of *a*-OEGMA ($M_n = 500$ g/mol) relative to the commercially available OEGMA ($M_n = 300$ g/mol) for drug delivery applications, we prepared both acidic pH-cleavable poly(ϵ -caprolactone)₂₁-*b*-poly(*a*-OEGMA)₁₁ (PCL₂₁-*b*-P(*a*-OEGMA)₁₁) and pH-insensitive analogues of PCL₂₁-*b*-P(OEGMA)₁₈ with an almost identical molecular weight (MW) of approximately 5.0 kDa for the hydrophilic blocks by a combination of ring-opening polymerization (ROP) of ϵ -CL and subsequent atom transfer radical polymerization (ATRP) of *a*-OEGMA or OEGMA. The pH-responsive micelles self-assembled from PCL₂₁-*b*-P(*a*-OEGMA)₁₁ showed sufficient salt stability, but efficient acidic pH-triggered aggregation that was confirmed by the DLS and TEM measurements as well as further characterizations of the products after degradation. *In vitro* drug release study revealed significantly promoted drug release at pH 5.0 relative to the release profile recorded at pH 7.4 due to the loss of colloidal stability and formation of micelle aggregates. The delivery efficacy evaluated by flow cytometry analyses and an *in vitro* cytotoxicity study in A549 cells further corroborated greater cellular uptake and cytotoxicity of Dox-loaded pH-sensitive micelles of

1
2
3 PCL₂₁-*b*-P(*a*-OEGMA)₁₁ relative to the pH-insensitive analogues of PCL₂₁-*b*-P(OEGMA)₁₈. This
4
5 study therefore presents a facile and robust means toward tumor acidic pH-responsive polymers
6
7 as well as provides a one solution to the tradeoff between extracellular stability and intracellular
8
9 high therapeutic efficacy of drug delivery systems using a novel monomer of *a*-OEGMA with
10
11 dual functionalities.
12
13
14
15
16
17
18
19
20
21
22
23
24
25
26
27
28
29
30
31
32
33
34
35
36
37
38
39
40
41
42
43
44
45
46
47
48
49
50
51
52
53
54
55
56
57
58
59
60

Introduction

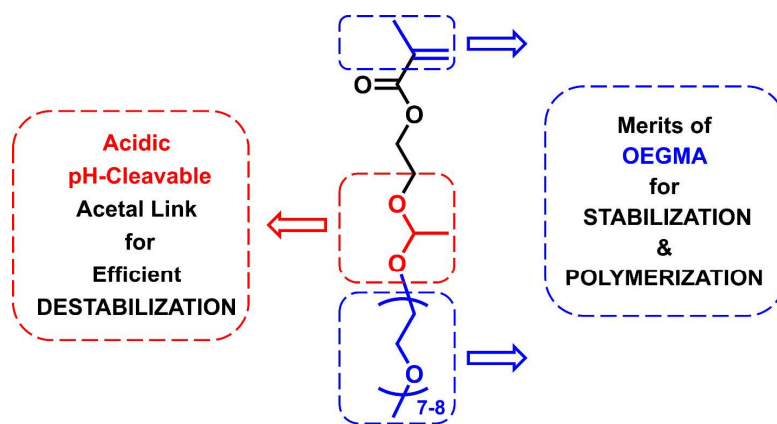
In the past several decades, stimuli-responsive polymers capable of responding to various bio-relevant triggers including pH, temperature, and redox potential for structural change or dissociation toward enhanced intracellular therapeutic efficacy have drawn great attention.¹⁻¹⁰ More recently, the development of light-sensitive polymers¹¹⁻¹³ and nanodiamond (ND)@polymer hybrid systems¹⁴⁻¹⁷ have emerged as innovative platforms toward improved efficacy and safety of cancer nanomedicine applications.

Due to the notable pH gradients between the normal and tumor tissues as well as in different cellular compartments, that is, pH 5.5–6.0 for endosomes and pH 4.5–5.0 for lysosomes, while the extracellular pH of tumor microenvironment is pH 6.8, which is slightly lower than the physiological pH 7.4,¹⁸⁻²⁰ various pH-sensitive polymeric carriers containing acidic pH-cleavable links, such as acetal,²¹⁻²³ hydrazone,²⁴⁻²⁶ orthoester,^{27,28} and carbamate²⁹ have been successfully designed and synthesized to realize efficiently intracellular deformation of carriers and subsequently promoted release of loaded cargoes.

Although tremendous progresses have been made in this field of research, the preparation of tumor acidic pH-cleavable polymers generally requires tedious post-polymerization modifications, leading to batch-to-batch variation and scale-up complexity.^{30,31} Specifically, it remains a synthetic challenge to develop polymers containing multiple acid-cleavable links with readily and precisely modulated polymer composition and functionalities. For this purpose, we reported in this study a facile and universal strategy by designing and successfully synthesizing a dual functional monomer, *a*-OEGMA that bridges a methacrylate structure and oligo(ethylene glycol) (OEG) units via an acidic pH-cleavable acetal link (**Scheme 1**). Therefore the dual functions of *a*-OEGMA lies in (i) the merits of commercially available oligo(ethylene glycol)

1
2
3 monomethyl ether methacrylate (OEGMA) monomer, *i.e.*, hydrophilicity for extracellular
4 stabilization of particulates and a polymerizable methacrylate for adopting controlled living
5 radical polymerization (CLRP), and (ii) an acidic pH-cleavable acetal link^{30,31} for efficiently
6 intracellular destabilization of polymeric carries.
7
8
9

10
11
12 To demonstrate the advantages of *a*-OEGMA ($M_n = 500$ g/mol) relative to the commercially
13 available OEGMA ($M_n = 300$ g/mol) for drug delivery applications, we prepared both acidic pH-
14 cleavable poly(ϵ -caprolactone)₂₁-*b*-poly(*a*-OEGMA)₁₁ (PCL₂₁-*b*-P(*a*-OEGMA)₁₁) and pH-
15 insensitive analogues of PCL₂₁-*b*-P(OEGMA)₁₈ with an almost identical molecular weight (MW)
16 of approximately 5.0 kDa for the hydrophilic blocks, which was shown in our previous study³² to
17 provide sufficient stability for the self-assembled micelles, by a combination of ring-opening
18 polymerization (ROP) of ϵ -CL and subsequent atom transfer radical polymerization (ATRP) of
19 *a*-OEGMA or OEGMA. The delivery efficacy of acidic pH-cleavable micelles was evaluated by
20 an *in vitro* drug release study, confocal microscopy measurements, flow cytometry analyses as
21 well as an *in vitro* cytotoxicity study, and compared with the pH-insensitive analogues.
22
23
24
25
26
27
28
29
30
31
32
33
34



49 A Dual Functional Monomer 50 *a*-OEGMA 51

52 **Scheme 1.** Schematic illustration of structure and merits of *a*-OEGMA monomer developed in
53 this study.
54
55
56
57
58
59
60

Experimental Section

Materials, polymer synthesis and characterizations, *in vitro* drug loading and drug release study, and *in vitro* biological assays are provided in the supporting information (SI).

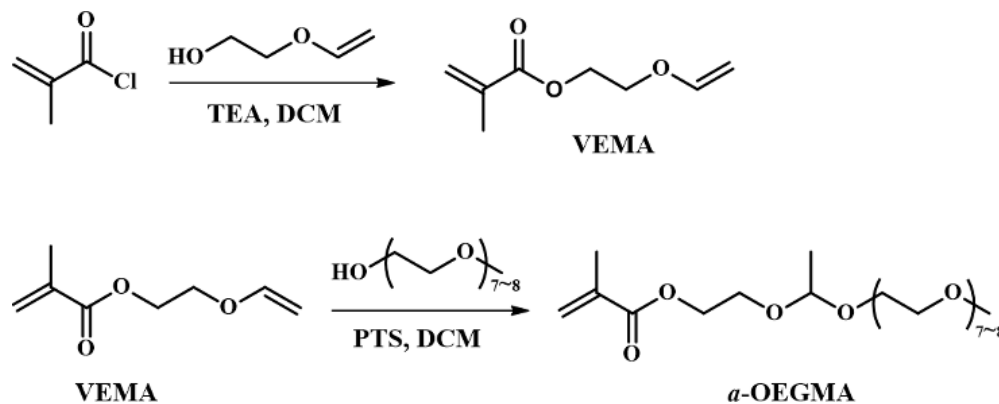
Synthesis of 2-(vinylloxy)ethyl methacrylate (VEMA)

VEMA was prepared from 2-(vinylloxy)ethanol and methacryloyl chloride in the presence of triethylamine (TEA).³³ Briefly, 2-(vinylloxy)ethanol (6.281 mL, 70 mmol), TEA (9.730 mL, 70 mmol) was dissolved in 100 mL of anhydrous DCM. A solution of methacryloyl chloride (6.159 mL, 63.64 mmol) in anhydrous DCM was added dropwise to the above mixture at 0°C under N₂ flow with stirring for a period of 30 min. Then the reaction mixture was further stirred at room temperature for 4 h. After reaction, a white byproduct TEA·HCl was filtrated out. The crude product was concentrated and purified by column chromatography with eluents of ethyl acetate/hexane (1/30, v/v) to obtain 8.30 g of colorless liquid (yield, 84%). ¹H NMR (400 MHz, CDCl₃, ppm, **Figure S1**): δ 6.51 (dd, *J* = 14.4, 6.8 Hz, 1H), 6.15 (s, 1H), 5.59 (s, 1H), 4.40 – 4.37 (m, 2H), 4.24 (dd, *J* = 14.0, 2.0 Hz, 1H), 4.06 (dd, *J* = 6.8, 2.4 Hz, 1H), 3.95 – 3.93 (m, 2H), 1.95 (s, 3H).

Synthesis of *a*-OEGMA (Scheme 2)

a-OEGMA was prepared from VEMA and mPEG (*M*_n = 350 g/mol) in the presence of a small catalytic amount of PTS according to the reported procedures.³⁴ Briefly, VEMA (4.685 g, 30 mmol), mPEG (10.50 g, 30 mmol), PTS (114.13 mg, 0.6 mmol) was dissolved in 60 mL of anhydrous DCM at room temperature under N₂ flow with stirring for a period of 30 min. The

reaction mixture was later stirred at 35°C for 3 days. After reaction, the reaction mixture was concentrated, and further purified by column chromatography with eluents of ethyl acetate/hexane (1/2, v/v) to obtain 11.08 g of colorless liquid (yield, 73%).



Scheme 2. Synthesis of a dual functional monomer, *a*-OEGMA.

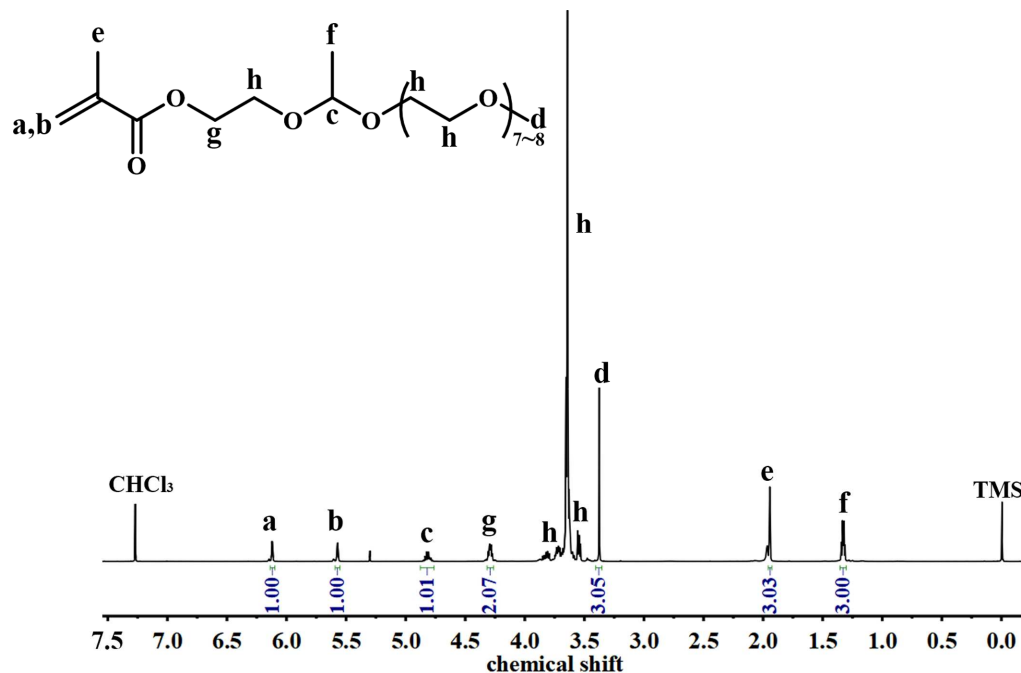
Results and Discussion

Synthesis of PCL-*b*-P(*a*-OEGMA)

The vinyloxy group of VEMA, which acts as an “anchor” site, could be functionalized by alcohols,³⁵ polyols,³⁶ and triazoles³⁷ to generate various functional methacryloyloxy acetals as promising monomers, comonomers, cross-linking agents, building blocks, and starting materials for the synthesis of biologically active substances, therefore VEMA was used as a precursor for *a*-OEGMA monomer in this study.

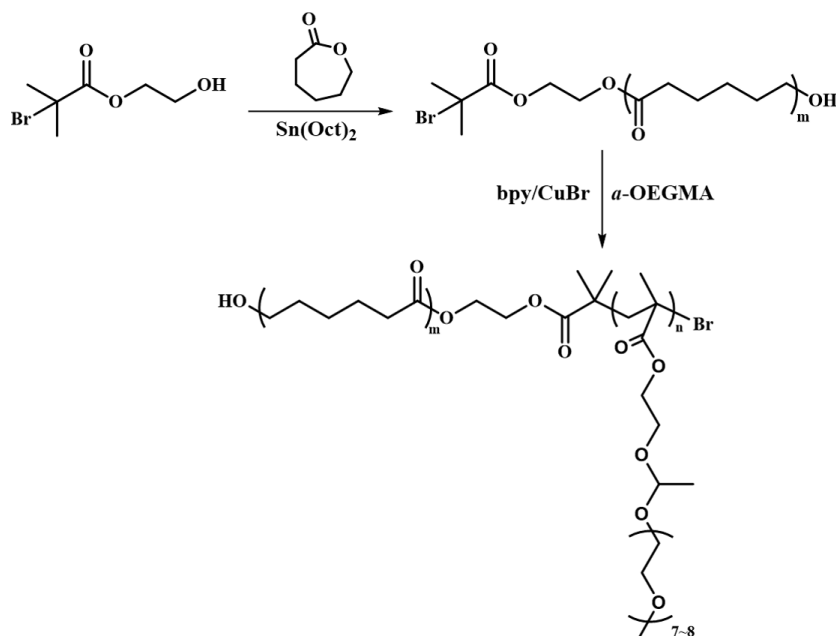
Successful synthesis of *a*-OEGMA monomer is confirmed by ¹H NMR analysis (**Figure 1**), which reveals the presence of all the characteristic signals of each proton including peak a and b at 6.12 and 5.57 ppm attributed to the vinyl protons of VEMA, peak d at 3.35 ppm assigned to PEG units, and peak c and f at 4.84-4.79, and 1.34-1.31 ppm attributable to the protons of acetal methine and adjacent methyl. More importantly, the ratio of the integrated intensity of peak g to f was calculated to be 2/3, strongly supporting equivalent coupling of VEMA and mPEG. Further

1
2
3 characterizations of *a*-OEGMA also confirm its successful synthesis including the appearance of
4 a characteristic signal at 99.8 ppm attributed to the acetal link in ^{13}C NMR spectrum (**Figure S2**),
5
6 the presence of all the characteristic absorbance bands in the FT-IR spectrum (**Figure S3**), and
7
8 the distribution of molecular ion peaks recorded in the high resolution mass spectrum (HRMS)
9
10
11
12
13 (**Figure S4**).



36
37 **Figure 1.** ^1H NMR spectrum of *a*-OEGMA in CDCl_3 .

38
39
40
41 To investigate the utility of this new monomer for polymer construction, *a*-OEGMA was next
42 used to prepare target acidic pH-cleavable amphiphilic diblock copolymer, PCL-*b*-P(*a*-OEGMA)
43 by ATRP using ROP-generated PCL-*i*BuBr as a macroinitiator (**Scheme 3**). The degree of
44 polymerization (DP) of PCL was first determined to be 21 by ^1H NMR analysis (**Figure S5**).
45
46
47
48
49
50
51
52
53
54
55
56
57
58
59
60



Scheme 3. Synthesis of acidic pH-cleavable diblock copolymer, PCL-*b*-P(*a*-OEGMA) by integrated ROP and ATRP.

To evaluate the polymerization properties of *a*-OEGMA by ATRP, a series of polymers was synthesized by varying polymerization time. The molecular parameters of the resulting PCL-*b*-P(*a*-OEGMA)s were summarized in **Table 1**. Taking PCL₂₁-*b*-P(*a*-OEGMA)₁₁ (Run 3 in **Table 1**) as an example, the DP of *a*-OEGMA was determined to be 11 by comparing the ratio of integrated intensity of peak f attributed to acetal methine to that of peak d assigned to PCL units (**Figure 2a**). All the three polymers show unimodal and symmetrical SEC elution peaks as well as a clear shift of the SEC elution traces toward higher molecular weight with increasing polymerization time (**Figure 2b**), which demonstrates well-controlled chain extension of *a*-OEGMA by ATRP. The precisely controlled polymerizations of *a*-OEGMA by CLRTP technique are reflected by the pseudo-first-order kinetics (**Figure 2c**) and narrow PDI (< 1.3) (**Table 1**) during the polymerization process, which offers a robust route toward acidic pH-cleavable hydrophilic building block.

Table 1. Summary of a series of PCL-*b*-P(*a*-OEGMA) polymers prepared at different polymerization time using PCL₂₁ as a macro-initiator.

run	Time (h) ^a	DP ^b	M_n^b (kDa)	M_n^c (kDa)	PDI ^c
1	1.5	4	4.31	5.48	1.23
2	2.5	8	6.33	7.64	1.28
3	3.5	11	7.85	10.8	1.26
4	2.0	18	7.69	13.3	1.32

^a Polymerization conditions, [*a*-OEGMA]₀: [PCL]₀: [bpy]₀: [CuBr]₀= 20: 1: 2: 1, [OEGMA]₀= 0.5 mol/L in anisole for run 1, 2 and 3. [OEGMA]₀: [PCL]₀: [bpy]₀: [CuBr]₀= 30: 1: 2: 1, [OEGMA]₀= 0.5 mol/L in anisole for run 4

^b Determined by ¹H NMR analysis

^c Determined by SEC-MALLS

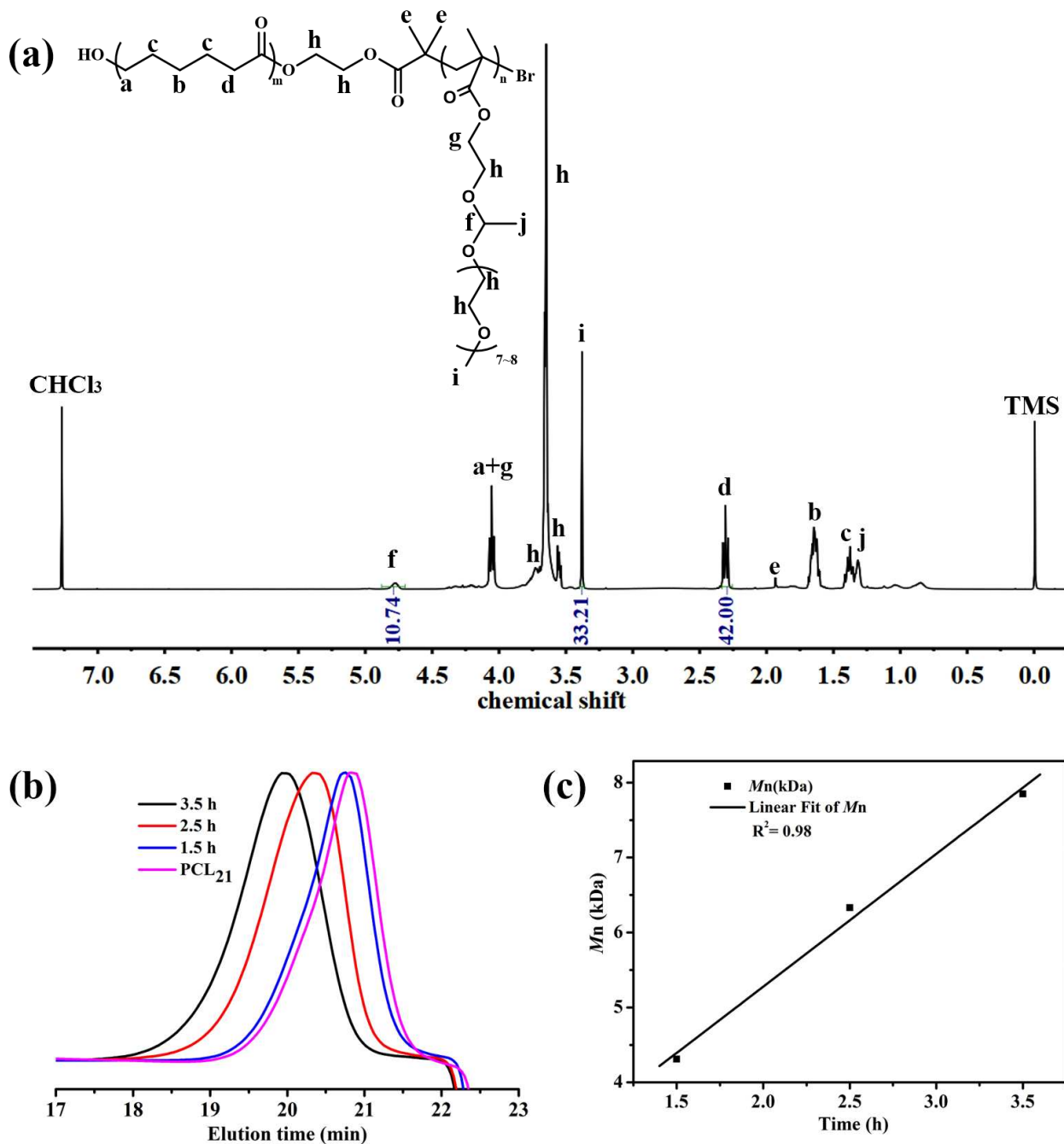


Figure 2. (a) ^1H NMR spectrum of $\text{PCL}_{21}\text{-}b\text{-P}(a\text{-OEGMA})_{11}$ in CDCl_3 . (b) SEC elution traces of $\text{PCL}_{21}\text{-iBuBr}$ and $\text{PCL-}b\text{-P}(a\text{-OEGMA})$ prepared at different polymerization time (eluent: DMF) (c) ATRP pseudo-first-order kinetics plot of $\text{PCL-}b\text{-P}(a\text{-OEGMA})$.

To demonstrate the advantages of *a*-OEGMA relative to the commercially available OEGMA for drug delivery applications, PCL₂₁-*b*-P(OEGMA)₁₈ diblock copolymer (**Figure S6** and **3**, Run 4 in **Table 1**) with an almost identical MW for the hydrophilic block was also prepared as a pH-insensitive analogue using the commercially available OEGMA monomer ($M_n = 300$ g/mol and 4~5 pendent EO units).

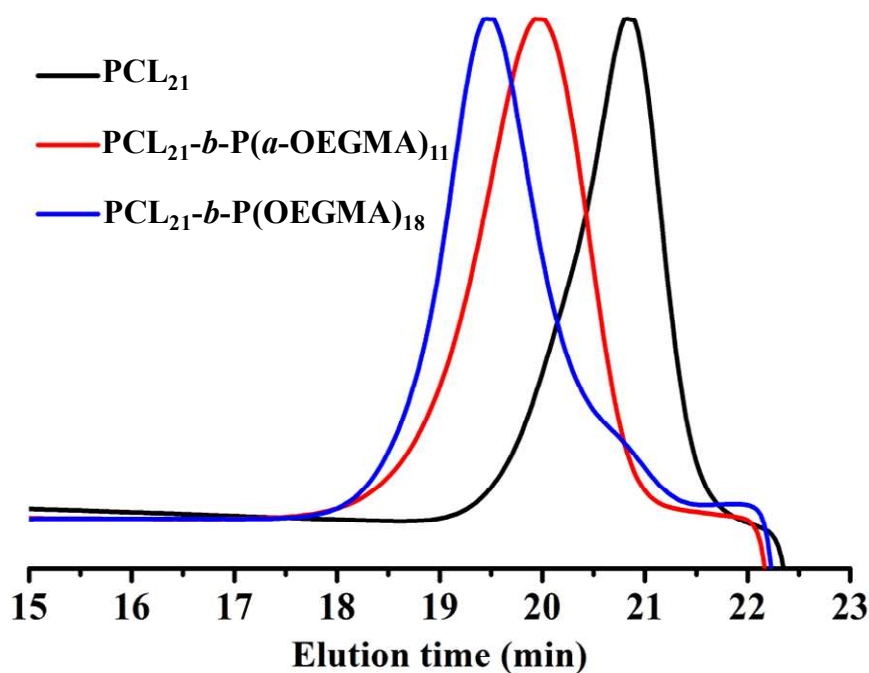


Figure 3. SEC elution traces of PCL, and PCL₂₁-*b*-P(*a*-OEGMA)₁₁ and PCL₂₁-*b*-P(OEGMA)₁₈ using DMF as an eluent.

Characterization of PCL₂₁-*b*-P(*a*-OEGMA)₁₁ micelles

The CMC of PCL₂₁-*b*-P(*a*-OEGMA)₁₁ was investigated using pyrene as a fluorescence probe. The fluorescence intensity keeps relatively constant at low concentrations, but increases dramatically at a certain concentration, indicating the formation of micelles. Such concentration was determined to be 9.33 mg/L for PCL₂₁-*b*-P(*a*-OEGMA)₁₁ (**Figure S7**) and 7.98 mg/L for

1
2
3 PCL₂₁-*b*-P(OEGMA)₁₈ (**Figure S8**). The slightly lower CMC value of PCL-*b*-P(OEGMA)₁₈
4 relative to that of PCL-*b*-P(*a*-OEGMA)₁₁ implies the greater thermodynamic stability³⁸ of pH-
5 insensitive micelles over pH-sensitive ones, which results likely from the different packing
6 behaviors³⁸⁻⁴⁰ caused by the hydrophilic POEGMA moiety with different DPs and brush-like
7 structures, *i.e.*, P(*a*-OEGMA)₁₁ with long OEG brush and short DP vs P(OEGMA)₁₈ with short
8 OEG brush and long DP, albeit their almost identical MW.

9
10
11 To evaluate the stability of self-assembled micelles, DLS was next used to determine the
12 average hydrodynamic size of micelles self-assembled by PCL₂₁-*b*-P(*a*-OEGMA)₁₁ and PCL₂₁-*b*-
13 P(OEGMA)₁₈ in both ddH₂O and PBS (pH 7.4, 150 mM) at various polymer concentrations. The
14 mean size recorded at different polymer concentrations ranges from approximately 110 to 150
15 nm (**Figure S9** and **S10**). Such change is most likely relevant to the different aggregation number
16 of polymer chains for micelle formation at various polymer concentrations above the CMC.
17 Therefore the largest size at 0.5 mg/mL of all the three concentrations probably results from the
18 greatest aggregation number at this concentration. However, the statistical insignificance
19 between each value implies the stability of both micelle formulations in salt medium and in
20 diluted conditions.

21
22
23 The morphology of micelles self-assembled by PCL₂₁-*b*-P(*a*-OEGMA)₁₁ and PCL₂₁-*b*-
24 P(OEGMA)₁₈ was visualized by TEM. Both polymers self-assembled into uniform nanoparticles
25 with regularly spherical shape (**Figure 4a** and **S11**) and similar dimension in a dried state. The
26 difference of the particle size between TEM and DLS measurements could be ascribed to the
27 hydration effect, that is, the hydrophilic PEG segments are solvated in an aqueous phase and can
28 be determined by DLS measurements but difficult to be observed under TEM observation.

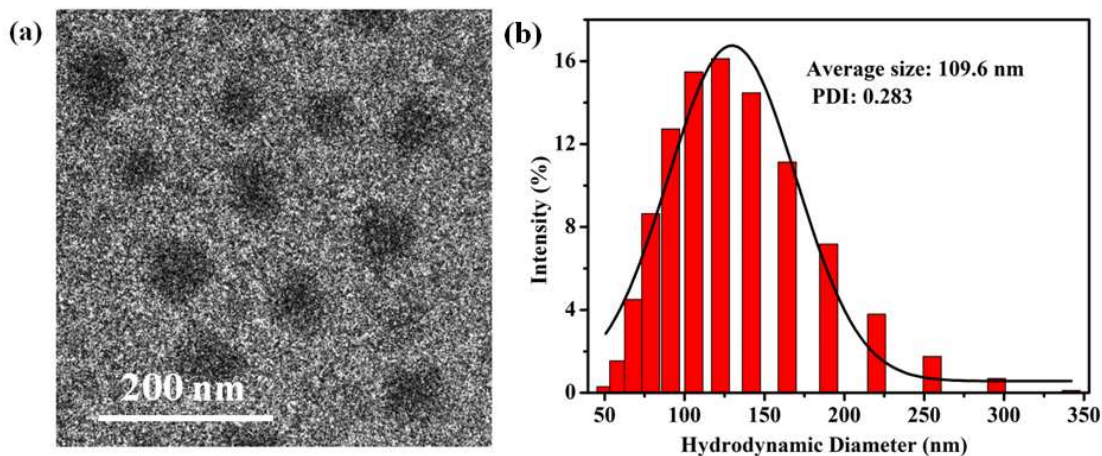


Figure 4. TEM image (a) and size distribution (b) of $\text{PCL}_{21}\text{-}b\text{-P}(a\text{-OEGMA})_{11}$ micelles at a polymer concentration of 0.5 mg/mL.

Acidic pH-triggered aggregation of $\text{PCL}_{21}\text{-}b\text{-P}(a\text{-OEGMA})_{11}$ micelles

To verify the acidic pH-triggered cleavage of acetal links, the size change of $\text{PCL}_{21}\text{-}b\text{-P}(a\text{-OEGMA})_{11}$ micelles incubated at different pH values of 7.4, 6.8 and 5.0 for various periods was monitored by DLS (**Figure 5a**).

The micelle size increased slightly from 118.5 to 143.9 nm after incubation at pH 7.4 for 48 h, however, such change is statistical insignificant, which implies the colloidal stability of the self-assembled micelles at the physiological pH.

In addition to the stability required at pH 7.4 for realizing long circulation, polymeric micelles must maintain certain structural integrity in the extracellular tumor microenvironment with a weakly acidic pH of 6.8 to facilitate efficiently cellular uptake. The micelles were thus incubated at pH 6.8 to evaluate the stability under this circumstance. The mean size kept almost stable around approximately 140 nm after incubation for 12 h, and reached a plateau of 220 nm with further incubation of 24 and 72 h. Such increase of micelle size is likely relevant to the minority cleavage of the acetal links, leading to a slight aggregation of the micelles.

1
2
3 However, incubation at pH 5.0 significantly promotes disassembly of micelles, which is
4 reflected by the dramatically increased size and a broader size distribution. Notably, a bimodal
5 distribution was clearly recorded for 48 h. The main population centered at approximately 504
6 nm probably implies the majority of the self-assembled micelles have been subjected to acidic
7 pH-triggered hydrolysis of acetal links and significant aggregation due to the deshielidng of
8 stabilizing corona composed of pendant OEG brushes. A few micelles remain intact, as
9 evidenced by the appearance of a small population centered at 122 nm, which is close to the
10 mean size of the stable micelles (**Figure 4b**). The disappearance of this small population as well
11 as similarly recorded mean sizes for prolonged incubation time of 72 and 96 h probably indicate
12 the complete hydrolysis within 72 h.
13
14
15
16
17
18
19
20
21
22
23
24
25

26 To confirm the size variation monitored by DLS, TEM observation of PCL₂₁-*b*-P(*a*-
27 OEGMA)₁₁ micelles after incubation at pH 6.8 and 5.0 for 24 h was performed (**Figure S12a** and
28 **b**). Well-dispersed micelles with regularly spherical shape and uniform size were maintained
29 even after incubation at pH 6.8 for 24 h (**Figure S12a**), demonstrating the stability of pH-
30 sensitive micelles at the pH of tumor microenvironment. The slightly increased size compared to
31 that observed in water (**Figure 4a**) is most likely due to the minority cleavage of the acetal links
32 in the micelle structure, which exerts negligible effect on the stability of the self-assembled
33 micelles. However, incubation at pH 5.0 for 24 h led to formation of densely arranged micelle
34 aggregates with irregularly spherical shape and nonuniform dimension (**Figure S12b**). More
35 importantly, the formation of aggregates is strongly evidenced by a significantly increased mean
36 size and broader size distribution at pH 5.0 relative to those observed in water and pH 6.8 as well
37 as the clearly visualized coalescences of individual small micelles. Taken together, the TEM
38
39
40
41
42
43
44
45
46
47
48
49
50
51
52
53
54
55
56
57
58
59
60

1
2
3 results are in good agreement with the DLS data, confirming the stability of pH-sensitive
4 micelles at pH 6.8, and occurrence of aggregation at pH 5.0.

5
6
7
8 ^1H NMR analysis was also utilized to verify the acidic pH-triggered hydrolysis of acetal links.
9
10 10 mg of $\text{PCL}_{21}\text{-}b\text{-P}(a\text{-OEGMA})_{11}$ was first dissolved in 4.5 mL of H_2O followed by addition of
11 hydrochloric acid aqueous solution (36 wt%, 1 mL) and stirred at 25 °C for 24 h. Note that the
12 transparent polymer solution became cloudy gradually, likely due to the detachment of
13 stabilizing pendant OEG brushes and significantly reduced solubility of the degraded products.
14
15 The mixture was finally freeze-dried and subjected to ^1H NMR analysis (**Figure 5b**), which
16 reveals presence of characteristic signals of PEG and PCL moieties, but complete loss of
17 characteristic peaks of acetal links at δ 4.79–4.84 ppm (highlighted using green color and arrow
18 in the structural formula and ^1H NMR spectrum, respectively). The results support acid-cleavage
19 of acetal links in $\text{PCL}_{21}\text{-}b\text{-P}(a\text{-OEGMA})_{11}$.

20
21
22
23
24
25
26
27
28
29
30
31 In addition, SEC-MALLS analyses were used to determine the MW of the degraded products.
32
33 The water-insoluble precipitates were collected by filtration and subjected to vacuum-drying
34 prior to SEC-MALLS measurements. As expected, the degraded products without pendant OEG
35 brushes show significantly decreased MW relative to the parent $\text{PCL}_{21}\text{-}b\text{-P}(a\text{-OEGMA})_{11}$, and
36 slightly increased MW compared to $\text{PCL}_{21}\text{-iBuBr}$ (**Figure 5c**), which confirms the scission of
37 acetal links rather than the hydrolysis of polyester under acidic condition.

38
39
40
41
42
43
44
45 To further provide an insight into the acidic-pH triggered degradation of $\text{PCL}_{21}\text{-}b\text{-P}(a\text{-}$
46 $\text{OEGMA})_{11}$, the fully degraded product, $\text{PCL}_{21}\text{-}b\text{-P}(2\text{-hydroxyethyl methacrylate})_{11}$ ($\text{PCL}_{21}\text{-}b\text{-}$
47 P(HEMA)_{11}) was also synthesized by ATRP of HEMA using $\text{PCL}_{21}\text{-iBuBr}$ macroinitiator given
48 that the full degradation of the hydrophilic $\text{P}(a\text{-OEGMA})$ block generates the P(HEMA) moiety
49 with somewhat hydrophilicity. The successful synthesis of $\text{PCL}_{21}\text{-}b\text{-P(HEMA)}_{11}$ with desired
50
51
52
53
54
55
56
57
58
59
60

1
2
3 polymer composition was confirmed by ^1H NMR (**Figure S13**) and SEC-MALLS (**Figure S14**)
4 analyses. The average size of the self-assemblies formed by $\text{PCL}_{21}\text{-}b\text{-P(HEMA)}_{11}$ was
5 determined by DLS to be 422.6 and 467.7 nm in water and PBS (pH 7.4), respectively (**Figure**
6 **S15**), which probably indicates the formation of large micelle aggregates due to the significantly
7 decreased hydrophilicity of P(HEMA) block relative to P(*a*-OEGMA) segment. TEM
8 observation of $\text{PCL}_{21}\text{-}b\text{-P(HEMA)}_{11}$ reveals dense arrangement of nanoparticles with irregularly
9 spherical shape and nonuniform size (**Figure S12c**), further confirming self-assembly of $\text{PCL}_{21}\text{-}$
10 $b\text{-P(HEMA)}_{11}$ into unstable aggregates. The results agree well with the acidic pH-triggered
11 aggregation of $\text{PCL}_{21}\text{-}b\text{-P}(a\text{-OEGMA)}_{11}$ micelles revealed by DLS (**Figure 5a**) and TEM
12 (**Figure S12b**) measurements.
13
14
15
16
17
18
19
20
21
22
23
24
25
26
27
28
29
30
31
32
33
34
35
36
37
38
39
40
41
42
43
44
45
46
47
48
49
50
51
52
53
54
55
56
57
58
59
60

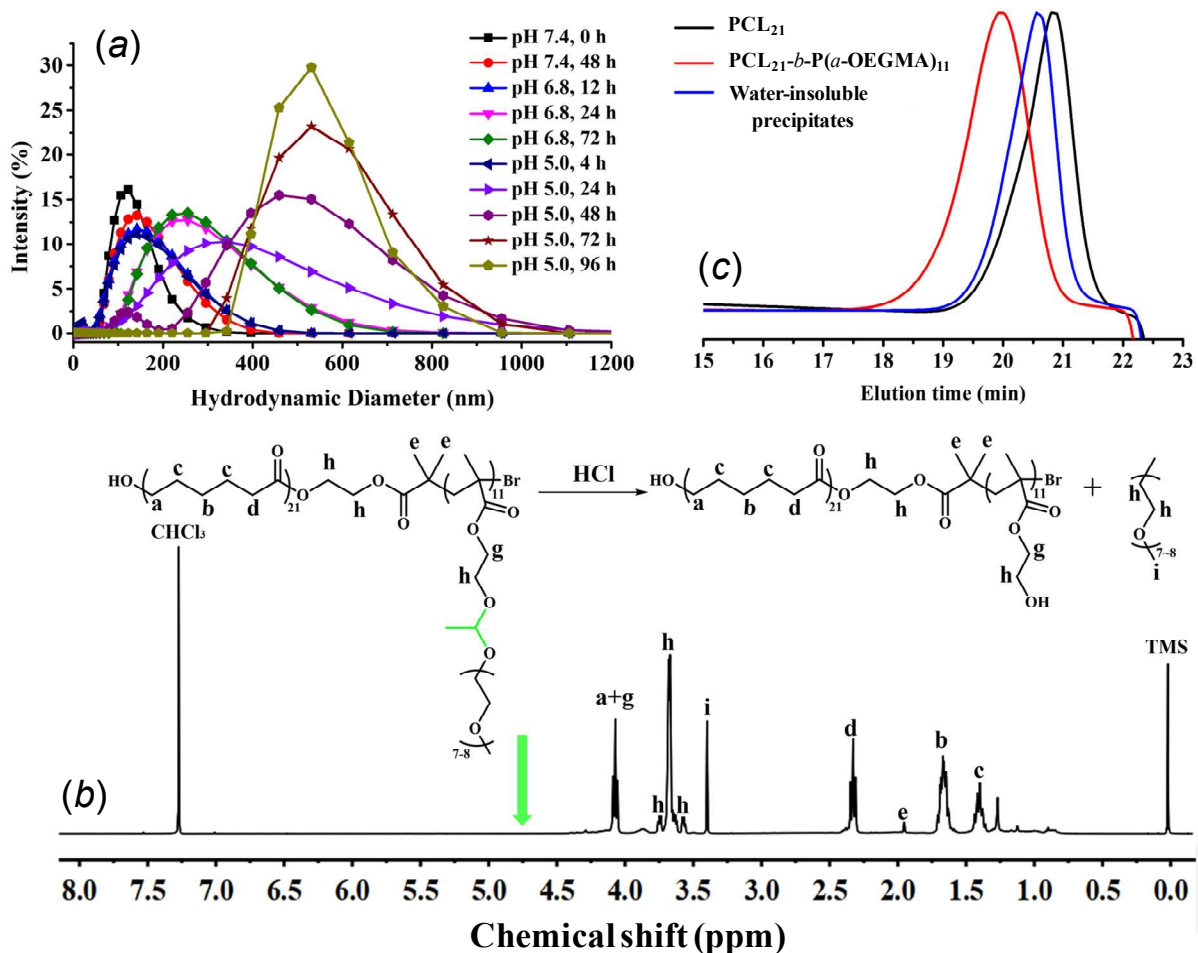


Figure 5. (a) DLS-monitored size change of PCL₂₁-b-P(a-OEGMA)₁₁ micelles after incubation at different pH values of 7.4, 6.8 and 5.0 for various periods at a polymer concentration of 0.25 mg/mL. (b) ¹H NMR spectrum of the degraded products of PCL₂₁-b-P(a-OEGMA)₁₁ treated with hydrochloric acid in CDCl₃. (c) SEC elution traces of PCL₂₁-iBuBr, PCL₂₁-b-P(a-OEGMA)₁₁, and water-insoluble precipitates after degradation of PCL₂₁-b-P(a-OEGMA)₁₁ by hydrochloric acid.

***In vitro* drug loading and drug release study**

1
2
3 Dox was chosen as a modal drug and encapsulated in PCL₂₁-*b*-P(*a*-OEGMA)₁₁ and PCL₂₁-*b*-
4 P(OEGMA)₁₈ micelles by dialysis method. The slightly lower CMC value and greater stability of
5 PCL-*b*-P(OEGMA)₁₈ micelles relative to PCL-*b*-P(*a*-OEGMA)₁₁ formulations contribute to the
6 smaller size and greater drug-loading capacity of PCL-*b*-P(OEGMA)₁₈ micelles (**Table 2**).
7
8
9

10
11
12 To validate the acidic pH-triggered drug release, *in vitro* drug release profiles were investigated
13 in buffer solutions with three different pHs of 7.4, 6.8, and 5.0, respectively (**Figure 6**). The
14 Dox-loaded PCL₂₁-*b*-P(*a*-OEGMA)₁₁ micelles showed almost identical drug release behaviors at
15 pH 7.4 and 6.8, demonstrating their apparent stability at the physiological pH and the pH of
16 tumor microenvironment. Shift of release medium from pH 7.4 or 6.8 to 5.0 promoted Dox
17 release from PCL₂₁-*b*-P(OEGMA)₁₈ micelles due to the increased solubility of protonated Dox
18 under the acidic conditions.^{41, 42} More importantly, nearly 90% of Dox was released at pH 5.0 for
19 Dox-loaded PCL₂₁-*b*-P(*a*-OEGMA)₁₁ micelles in 72 h, whereas approximately 50% Dox release
20 was recorded at pH 5.0 for Dox-loaded PCL₂₁-*b*-P(OEGMA)₁₈ micelles in the same period. The
21 significantly increased cumulative drug release is attributed to the acidic pH-triggered cleavage
22 of acetal links for efficient destabilization of PCL₂₁-*b*-P(*a*-OEGMA)₁₁ micelles and formation of
23 micelle aggregates toward promoted drug release.
24
25
26
27
28
29
30
31
32
33
34
35
36
37
38
39
40
41
42
43
44
45
46
47
48
49
50
51
52
53
54
55
56
57
58
59
60

Table 2. Summarized properties of blank and drug-loaded PCL₂₁-*b*-P(*a*-OEGMA)₁₁ and PCL₂₁-*b*-P(OEGMA)₁₈ micelles.

Micelle constructs	Size (nm)	PDI	CMC (mg/L)	DLC (%)	EE (%)
PCL ₂₁ - <i>b</i> -P(<i>a</i> -OEGMA) ₁₁	109.6	0.283	9.33	-	-
PCL ₂₁ - <i>b</i> -P(OEGMA) ₁₈	105.3	0.216	7.98	-	-
Dox-loaded PCL ₂₁ - <i>b</i> -P(<i>a</i> -OEGMA) ₁₁	147.6	0.250	-	5.76	5.88
Dox-loaded PCL ₂₁ - <i>b</i> -P(OEGMA) ₁₈	124.7	0.271	-	6.16	6.78

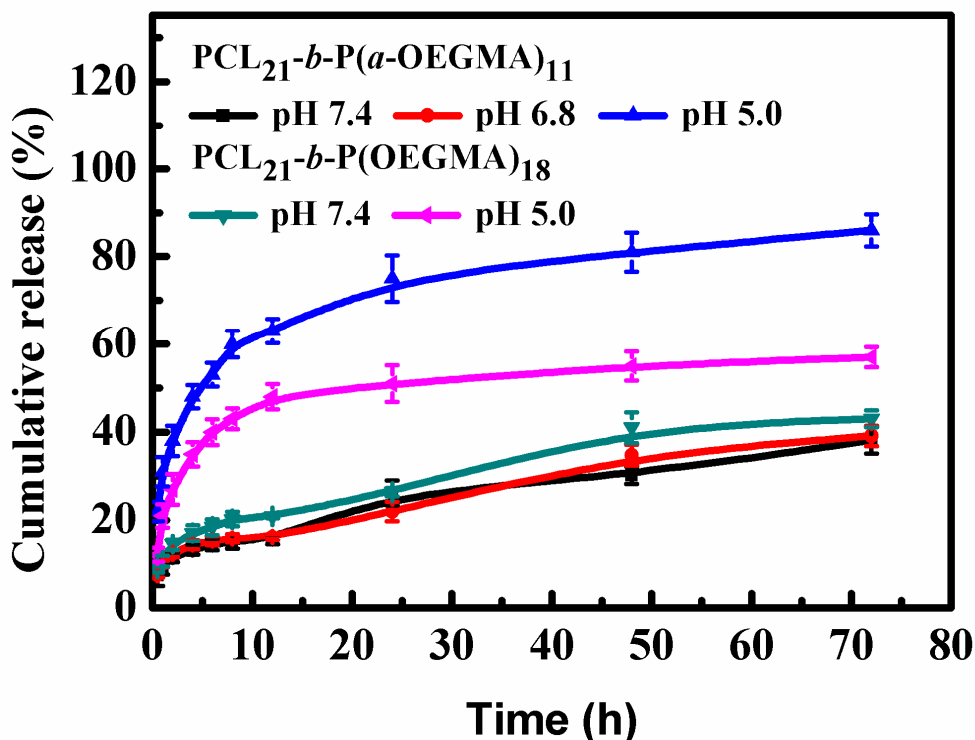


Figure 6. *In vitro* drug release profiles of Dox-loaded PCL₂₁-*b*-P(*a*-OEGMA)₁₁ and PCL₂₁-*b*-P(OEGMA)₁₈ micelles at different conditions.

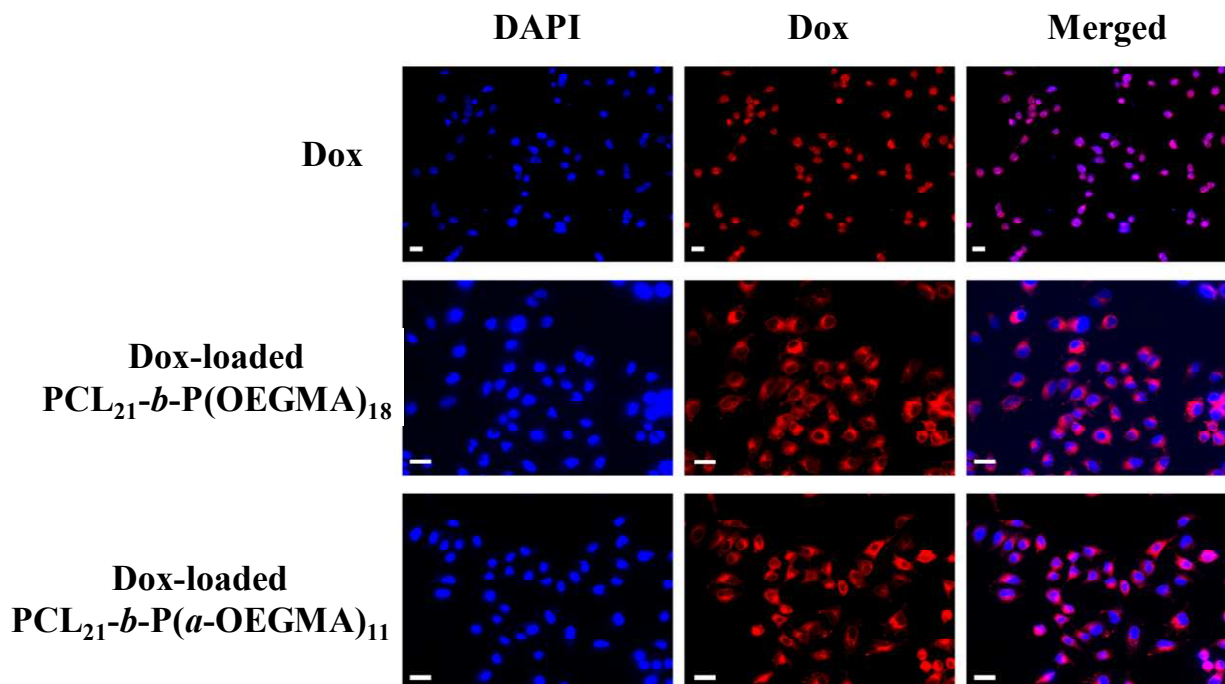
In vitro cellular uptake and cytotoxicity studies

Figure 7. Confocal imaging of free DOX (red), Dox-loaded PCL₂₁-b-P(OEGMA)₁₈ and PCL₂₁-b-P(*α*-OEGMA)₁₁ micelles uptake in A549 cells (nuclei stained blue with DAPI). Cells were treated with free DOX or polymer constructs at 25% of its IC₅₀ value to minimize cell death.

The cellular uptake efficiency was first evaluated using confocal microscopy. Dox fluorescence was clearly observed in the cytoplasm and/or nuclei of cells incubated with free Dox or both Dox-loaded micelles for 4 h (**Figure 7**), indicating that both micelle constructs can efficiently transport the anticancer drug to the cells and subsequently undergo intracellular trafficking. Then the cellular uptake was further quantified using flow cytometry (FCM) analyses (**Figure 8a**). The mean fluorescence intensity of A549 cells treated with both Dox-loaded micelles was clearly

1
2
3 observed in 4 h. The cells treated with free Dox presented much higher fluorescence intensity
4
5 than the cells incubated with micelle formulations most likely due to the faster diffusion rate of
6
7 Dox in cells with a mechanism of direct membrane permeation. Interestingly, the Dox-loaded
8
9 PCL₂₁-*b*-P(*a*-OEGMA)₁₁ micelles mediated slightly higher fluorescence intensity with statistical
10
11 significance relative to the pH-insensitive analogues, which probably implies the stronger ability
12
13 for the pH-sensitive micelles to deliver the anticancer drug into the cancer cells.
14
15

16
17 Finally, the cytotoxicity of Dox-loaded PCL₂₁-*b*-P(*a*-OEGMA)₁₁ and PCL₂₁-*b*-P(OEGMA)₁₈
18
19 micelles to A549 cells was assessed by 3-(4,5-dimethylthiazol-2-yl)-5-(3-
20
21 carboxymethoxyphenyl)-2-(4-sulfophenyl)-2H-tetrazolium (MTS) cell viability assay. Both
22
23 blank micelles were non-toxic to A549 cells up to a concentration of 3.8 mg/mL (**Figure 8b**).
24
25 The half maximal inhibitory concentration (IC₅₀) of free Dox, Dox-loaded PCL₂₁-*b*-P(*a*-
26
27 OEGMA)₁₁ and PCL₂₁-*b*-P(OEGMA)₁₈ micelles is 3.64 (3.13, 4.24), 128.5 (122.2, 135.1), and
28
29 194.7 (180.3, 210.3) μg/mL, respectively (**Figure 8c**). The increased IC₅₀ of Dox-loaded
30
31 micelles relative to free Dox is likely attributed to the slower internalization mechanism and the
32
33 release kinetics of free drug from the micelles. Most importantly, the Dox-loaded PCL₂₁-*b*-P(*a*-
34
35 OEGMA)₁₁ micelles showed significantly greater therapeutic efficacy, *i.e.*, lower IC₅₀ value than
36
37 the pH-insensitive counterparts due to the efficient destabilization and aggregation of micelles
38
39 and subsequently promoted drug release in the intracellular acidic pH environment.
40
41
42
43
44
45
46
47
48
49
50
51
52
53
54
55
56
57
58
59
60

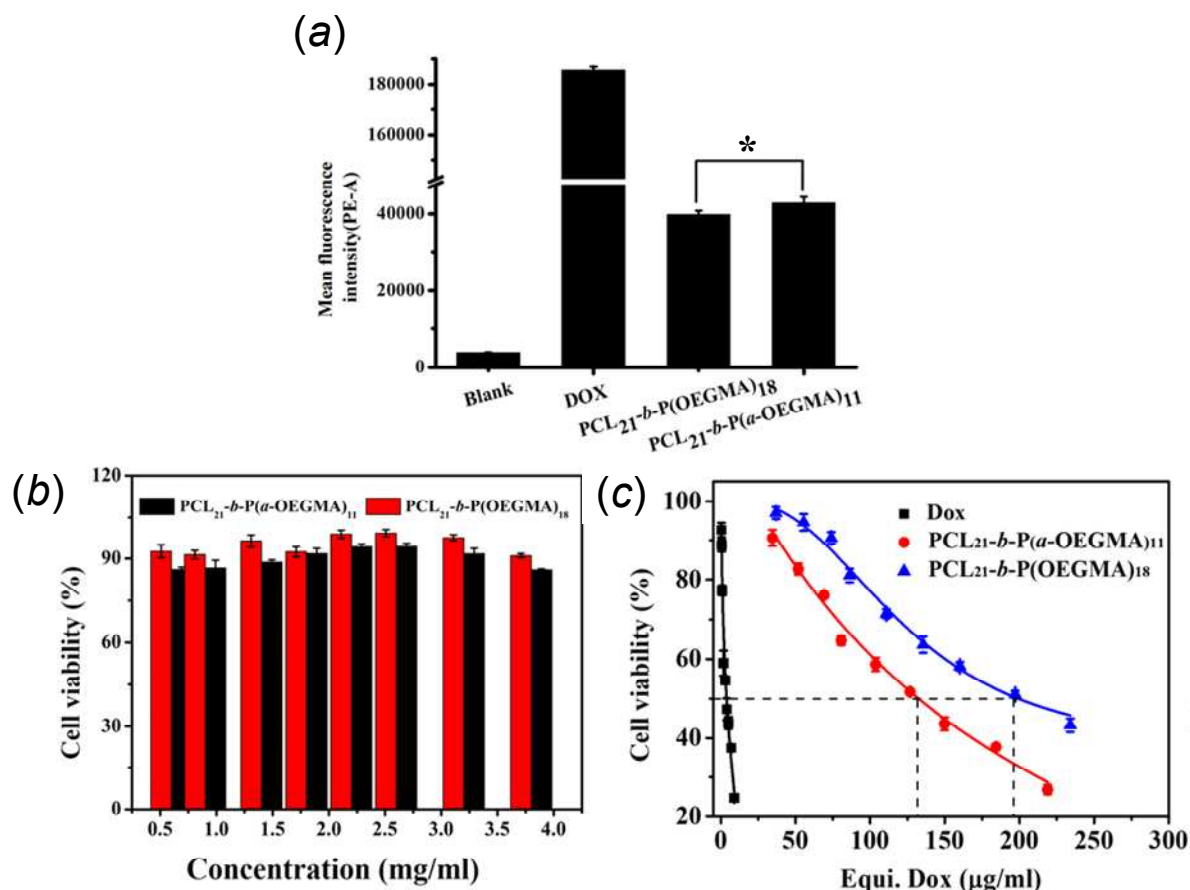


Figure 8. (a) Quantitative measurements of the mean fluorescence intensity after incubation with free Dox, Dox-loaded micelles of PCL₂₁-b-P(a-OEGMA)₁₁ and PCL₂₁-b-P(OEGMA)₁₈ in A549 cells via flow cytometry (4 h incubation, Dox concentration = 20 µg/mL, and 10000 cells were counted). The data were expressed as mean ± SD, n = 3 (**p* < 0.01). Viability of A549 cells exposed to (b) blank micelles of PCL₂₁-b-P(OEGMA)₁₈, PCL₂₁-b-P(a-OEGMA)₁₁ and (c) free Dox, Dox-loaded micelles of PCL₂₁-b-P(a-OEGMA)₁₁ and PCL₂₁-b-P(OEGMA)₁₈.

Conclusions

In summary, to develop a facile and universal alternative toward tumor acidic pH-responsive polymers, we reported in this study successful synthesis of a dual functional monomer, *a*-OEGMA that integrates the merits of commercially available OEGMA monomer for both extracellular stabilization of particulates and CLRP-mediated polymerization properties, and an acidic pH-cleavage acetal link for efficient intracellular destabilization of polymeric carriers. Amphiphilic block copolymers, PCL₂₁-*b*-P(*a*-OEGMA)₁₁ with pendant acidic pH-cleavable OEG brushes were further prepared using this monomer. The delivery efficacy evaluated by an *in vitro* drug release study, flow cytometry analyses as well as an *in vitro* cytotoxicity study further confirmed promoted drug release at pH 5.0, greater cellular uptake and cytotoxicity of Dox-loaded pH-sensitive micelles of PCL₂₁-*b*-P(*a*-OEGMA)₁₁ relative to the pH-insensitive analogues of PCL₂₁-*b*-P(OEGMA)₁₈. The *a*-OEGMA monomer developed herein therefore presents a facile and robust means toward tumor acidic pH-responsive polymers as well as provides a one solution to the tradeoff between extracellular stability and intracellular high therapeutic efficacy of drug delivery systems.

ASSOCIATED CONTENT

Experimental details, ¹H, ¹³C NMR, FT-IR, HRMS data of VEMA, ¹H NMR spectra of PCL-*i*BuBr, and PCL₂₁-*b*-P(OEGMA)₁₈, CMC determinations of PCL₂₁-*b*-P(*a*-OEGMA)₁₁ and PCL₂₁-*b*-P(OEGMA)₁₈, TEM images and size distributions of PCL₂₁-*b*-P(OEGMA)₁₈ micelles, average size of PCL₂₁-*b*-P(*a*-OEGMA)₁₁ and PCL₂₁-*b*-P(OEGMA)₁₈ micelles at various polymer concentrations in water and PBS (pH 7.4, 150 mM), TEM images of PCL₂₁-*b*-P(*a*-

1
2
3 OEGMA)₁₁ micelles after incubation at pH 6.8 and 5.0 for 24 h, and micelle aggregates formed
4
5 by PCL₂₁-*b*-P(HEMA)₁₁, ¹H NMR spectrum and SEC elution trace of PCL₂₁-*b*-P(HEMA)₁₁,
6
7 size distributions of PCL₂₁-*b*-P(HEMA)₁₁ in water and PBS (pH 7.4, 150 mM), standard curve of
8
9 Dox in PBS (pH 7.4) are available in Figure S1-S16.
10
11
12
13

14 **AUTHOR INFORMATION**

15
16
17 L. Zheng and X. Zhang contributed equally to this paper.
18
19
20

21 **Corresponding Authors**

22
23 weih@lzu.edu.cn (H. Wei)

24
25
26 1126@hbtcn.edu.cn (C. Chang)
27
28
29

30 **Notes**

31
32
33 The authors declare no competing financial interest.
34
35
36

37 **ORCID**

38
39
40 Hua Wei: 0000-0002-5139-9387
41
42
43

44 **ACKNOWLEDGMENT**

45
46
47 The authors acknowledge the financial support from the National Natural Science Foundation of
48
49 China (51473072 and 21504035), the Thousand Young Talent Program, and the Open Research
50
51 Fund of State Key Laboratory of Polymer Physics and Chemistry, Changchun Institute of
52
53 Applied Chemistry, Chinese Academy of Sciences.
54
55
56
57
58
59
60

References

- (1) Cayre, O. J.; Chagneux, N.; Biggs, S. Stimulus-Responsive Core-Shell Nanoparticles: Synthesis and Applications of Polymer Based Aqueous Systems. *Soft Matter* **2011**, *7*, 2211–2234.
- (2) Felber, A. E.; Dufresne, M. H.; Leroux, J. C. pH-Sensitive Vesicles, Polymeric Micelles, and Nanospheres Prepared with Polycarboxylates. *Adv. Drug Delivery Rev.* **2012**, *64*, 979–992.
- (3) Fleige, E.; Quadir M. A.; Haag, R. Stimuli-Responsive Polymeric Nanocarriers for the Controlled Transport of Active Compounds: Concepts and Applications. *Adv. Drug Delivery Rev.* **2012**, *64*, 866–884.
- (4) Tian, H. Y.; Tang, Z. H.; Zhuang, X. L.; Chen, X. S; Jing, X. B. Biodegradable Synthetic Polymers: Preparation, Functionalization and Biomedical Application. *Prog. Polym. Sci.* **2012**, *37*, 237–280.
- (5) Zhang, Q. N.; Ko, R.; Oh, J. K. Recent Advances in Stimuli-Responsive Degradable Block Copolymer Micelles: Synthesis and Controlled Drug Delivery Applications. *Chem. Commun.* **2012**, *48*, 7542–7552.
- (6) Wei, H.; Zhuo, R. X.; Zhang, X. Z. Design and Development of Polymeric Micelles with Cleavable Links for Intracellular Drug Delivery. *Prog. Polym. Sci.* **2013**, *38*, 503–535.
- (7) Binauld, S.; Scarano, W.; Stenzel, M. H. pH-Triggered Release of Platinum Drugs Conjugated to Micelles via an Acid-Cleavable Linker. *Macromolecules* **2012**, *45*, 6989–6999.
- (8) Jackson, A. W.; Fulton, D. A. Making Polymeric Nanoparticles Stimuli-Responsive with Dynamic Covalent Bonds. *Polym. Chem.* **2013**, *4*, 31–45.

- 1
2
3 (9) Huynh, V. T.; Binauld, S.; Souza, P. L.; Stenzel, M. H. Acid Degradable Cross-Linked
4 Micelles for the Delivery of Cisplatin: A Comparison with Nondegradable Cross-Linker. *Chem.*
5
6 *Mater.* **2012**, *24*, 3197–3211.
7
8
9
10 (10) Liu, X.; Tian, Z. C.; Chen C.; Allcock, H. R. UV-Cleavable Unimolecular Micelles:
11
12 Synthesis and Characterization toward Photocontrolled Drug Release Carriers. *Polym. Chem.*
13
14 **2013**, *4*, 1115–1125.
15
16
17 (11) Nishiyama, N.; Iriyama, A.; Jang, W. D.; Miyata, K.; Itaka, K.; Inoue, Y.; Takahashi, H.;
18
19 Yanagi, Y.; Tamaki, Y.; Koyama, H.; Kataoka, K. Light-Induced Gene Transfer from Packaged
20
21 DNA Enveloped in A Dendrimeric Photosensitizer. *Nat. Mater.* **2005**, *4*, 934–941.
22
23
24 (12) Founi, M. E.; Soliman, S. M. A.; Vanderesse, R.; Acherar, S.; Guedon, E.; Chevalot, I.;
25
26 Babin, J.; Six, J. L. Light-Sensitive Dextran-Covered PNBA Nanoparticles as Triggered Drug
27
28 Delivery Systems: Formulation, Characteristics and Cytotoxicity. *J. Colloid Interface Sci.* **2018**,
29
30 *514*, 289-298.
31
32
33 (13) Sun, C.; Ji. S.; Li, F.; Xu, H. Diselenide-Containing Hyperbranched Polymer with Light-
34
35 Induced Cytotoxicity. *ACS Appl. Mater. Interfaces*, **2017**, *9*, 12924–12929.
36
37
38 (14) Kim, H.; Man, H. B.; Saha, B.; Kopacz, A. M.; Lee, O. S.; Schatz, G. C.; Ho, D.; Liu, W. K.
39
40 Multiscale Simulation as A Framework for the Enhanced Design of Nanodiamond-
41
42 Polyethylenimine-Based Gene Delivery. *J. Phys. Chem. Lett.*, **2012**, *3*, 3791–3797.
43
44
45 (15) Vaijayanthimala, V.; Lee, D. K.; Kim, S. V.; Yen, Albert.; Tsai, N.; Ho, D.; Chang, H. C.;
46
47 Shenderova, O. Nanodiamond-Mediated Drug Delivery and Imaging: Challenges and
48
49 Opportunities. *Expert Opin. Drug Delivery* **2015**, *12*, 735-749.
50
51
52 (16) Lai, H.; Chen, F.; Lu, M.; Stenzel, M. H.; Xiao, P. Polypeptide-Grafted Nanodiamonds for
53
54 Controlled Release of Melittin to Treat Breast Cancer. *ACS Macro Lett.*, **2017**, *6*, 796–801.
55
56
57
58
59
60

- 1
2
3 (17) Zhao, J.; Lu, M.; Lai, H.; Lu, H.; Lalevée, J.; Barner-Kowollik, C.; Stenzel, M. H.; Xiao, P.
4
5 Delivery of Amonafide from Fructose-Coated Nanodiamonds by Oxime Ligation for the
6
7 Treatment of Human Breast Cancer. *Biomacromolecules*, **2018**, *19*, 481–489.
8
9
10 (18) Deng, C.; Jiang, Y. J.; Cheng, R.; Meng, F. H.; Zhong, Z. Y. Biodegradable Polymeric
11
12 Micelles for Targeted and Controlled Anticancer Drug Delivery: Promises, Progress and
13
14 Prospects. *Nano Today* **2012**, *7*, 467–480.
15
16
17 (19) Ganta, S.; Devalapally, H.; Shahiwala, A.; Amiji, M. A Review of Stimuli-Responsive
18
19 Nanocarriers for Drug and Gene Delivery. *J. Controlled Release* **2008**, *126*, 187–204.
20
21
22 (20) Lee, E. S.; Gao, Z. G.; Bae, Y. H. Recent Progress in Tumor pH Targeting Nanotechnology.
23
24 *J. Controlled Release* **2008**, *132*, 164–170.
25
26
27 (21) Gillies, E. R.; Goodwin, A. P.; Fréchet, J. M. J. Acetals as pH-Sensitive Linkages for Drug
28
29 Delivery. *Bioconjugate Chem.* **2004**, *15*, 1254–1263.
30
31
32 (22) Jain, R.; Standley, S. M.; Fréchet, J. M. J. Synthesis and Degradation of pH-Sensitive Linear
33
34 Poly(amidoamine)s. *Macromolecules* **2007**, *40*, 452–457.
35
36
37 (23) Tonhauser, C.; Schüll, C.; Dingels, C.; Frey, H. Branched Acid-Degradable, Biocompatible
38
39 Polyether Copolymers via Anionic Ring-Opening Polymerization Using an Epoxide Inimer. *ACS*
40
41 *Macro Lett.* **2012**, *1*, 1094–1097.
42
43
44 (24) Bae, Y.; Fukushima, S.; Harada, A.; Kataoka, K. Design of Environment-Sensitive
45
46 Supramolecular Assemblies for Intracellular Drug Delivery: Polymeric Micelles that are
47
48 Responsive to Intracellular pH Change. *Angew. Chem., Int. Ed.* **2003**, *42*, 4640–4643.
49
50
51 (25) Zhu, L. J.; Tu, C. L.; Zhu, B. S.; Su, Y.; Pang, Y.; Yan, D. Y.; Wu, J. L.; Zhu, X. Y.
52
53 Construction and Application of pH-Triggered Cleavable Hyperbranched Polyacylhydrazone for
54
55 Drug Delivery. *Polym. Chem.* **2011**, *2*, 1761–1768.
56
57
58
59
60

- 1
2
3 (26) Du, J. Z.; Du, X. J.; Mao, C. Q.; Wang, J. Tailor-Made Dual pH-Sensitive Polymer
4 Doxorubicin Nanoparticles for Efficient Anticancer Drug Delivery. *J. Am. Chem. Soc.* **2011**,
5 *133*, 17560–17563.
6
7
8
9
10 (27) Cheng, J.; Ji, R.; Gao, S. J.; Du, F. S.; Li, Z. C. Facile Synthesis of Acid-Labile Polymers
11 with Pendent Ortho Esters. *Biomacromolecules* **2012**, *13*, 173–179.
12
13
14 (28) Heller, J.; Barr, J.; Ng, S. Y.; Abdellauoi, K. S.; Gurny, R. Poly(ortho esters): Synthesis,
15 Characterization, Properties and Uses. *Adv. Drug Delivery Rev.* **2002**, *54*, 1015–1039.
16
17
18
19 (29) Liu, T.; Li, X. J.; Qian, Y. F.; Hu, X. L.; Liu, S. Y. Multifunctional pH-Disintegrable
20 Micellar Nanoparticles of Asymmetrically Functionalized β -Cyclodextrin-Based Star Copolymer
21 Covalently Conjugated with Doxorubicin and DOTA-Gd Moieties. *Biomaterials* **2012**, *33*,
22 2521–2531.
23
24
25
26
27
28 (30) Wang, H. R.; He, J. L.; Zhang, M. Z.; Tao, Y. F.; Li, F.; Tamb, K. C.; Ni, P. H.
29 Biocompatible and Acid-Cleavable Poly(ϵ -Caprolactone)-Acetal-Poly(Ethylene Glycol)-Acetal-
30 Poly(ϵ -Caprolactone) Triblock Copolymers: Synthesis, Characterization and pH-Triggered
31 Doxorubicin Delivery. *J. Mater. Chem. B* **2013**, *1*, 6596–6607.
32
33
34
35
36
37 (31) Miao, K.; Shao, W.; Liu, H. H.; Zhao, Y. L. Synthesis and Properties of a Dually Cleavable
38 Graft Copolymer Comprising Pendant Acetal Linkages. *Polym. Chem.* **2014**, *5*, 1191–1201.
39
40
41
42 (32) Wei, H.; Pahang, J. A.; Pun, S. H. Optimization of Brush-Like Cationic Copolymers for
43 Nonviral Gene Delivery. *Biomacromolecules* **2013**, *14*, 275–284.
44
45
46
47 (33) Zhang, H. M.; Ruckenstei, E. Graft Copolymers by Combined Anionic and Cationic
48 Polymerizations Based on the Homopolymerization of a Bifunctional Monomer.
49 *Macromolecules* **1998**, *31*, 746–752.
50
51
52
53
54
55
56
57
58
59
60

- 1
2
3 (34) Kalourkoti, M. R.; Matyjaszewski K.; Patrickios, C. S. Synthesis, Characterization and
4 Thermolysis of Hyperbranched Homo- and Amphiphilic Co-Polymers Prepared Using an Inimer
5 Bearing a Thermolyzable Acylal Group. *Macromolecules* **2012**, *45*, 1313–1320.
6
7
8
9
10 (35) Aoshima, S.; Sugihara, S.; Shibayama, M.; Kanaoka, S. Synthesis and Self-Association of
11 Stimuli-Responsive Diblock Copolymers by Living Cationic Polymerization. *Macromol. Symp.*
12 **2004**, *215*, 151-164.
13
14
15
16 (36) Schild, H. G. Poly(*N*-isopropylacrylamide): Experiment, Theory and Application. *Prog.*
17 *Polym. Sci.* **1992**, *17*, 163-249.
18
19
20 (37) Hoffman, A. S. “Intelligent” Polymers in Medicine and Biotechnology. *Macromol. Symp.*
21 **1995**, *98*, 645-664.
22
23
24
25 (38) Wang, Y.; Wu, Z.; Ma, Z.; Tu, X.; Zhao, S.; Wang, B.; Ma, L.; Wei, H. Promotion of
26 Micelle Stability via a Cyclic Hydrophilic Moiety. *Polym. Chem.* **2018**, *9*, 2569-2573.
27
28
29 (39) Chu, Y.; Zhang, W.; Lu, X.; Mu, G.; Zhang, B.; Li, Y.; Cheng, S. Z. D.; Liu, T. Rational
30 Controlled Morphological Transitions in the Self-Assembled Multi-Headed Giant Surfactants in
31 Solution. *Chem. Commun.* **2016**, *52*, 8687-8690.
32
33
34
35 (40) Zhang, W.; Huang, M.; Su, H.; Zhang, S.; Yue, K.; Dong, X. H.; Li, X.; Liu, H.; Zhang, S.;
36 Wesdemiotis, C.; Lotz, B.; Zhang, W. B.; Li, Y.; Cheng, S. Z. D. Toward Controlled
37 Hierarchical Heterogeneities in Giant Molecules with Precisely Arranged Nano Building Blocks.
38 *ACS Cent. Sci.* **2016**, *2*, 48-54.
39
40
41 (41) Prabakaran, M.; Grailer, J. J.; Pilla, S.; Steeber D. A.; Gong, S. Q. Folate-Conjugated
42 Amphiphilic Hyperbranched Block Copolymers Based on Boltorn H40, Poly(L-lactide) and
43 Poly(ethylene glycol) for Tumor-Targeted Drug Delivery. *Biomaterials* **2009**, *30*, 3009-3019.
44
45
46
47
48
49
50
51
52
53
54
55
56
57
58
59
60

1
2
3 (42) Wang, M.; Zhang, X.; Peng, H.; Zhang, M.; Zhang, X.; Liu, Z.; Ma, L.; Wei, H.
4
5 Optimization of Amphiphilic Miktoarm Star Copolymers for Anticancer Drug Delivery. *ACS*
6
7 *Biomater. Sci. Eng.* **2018**, DOI: 10.1021/acsbiomaterials.8b00678.
8
9
10
11
12
13
14
15
16
17
18
19
20
21
22
23
24
25
26
27
28
29
30
31
32
33
34
35
36
37
38
39
40
41
42
43
44
45
46
47
48
49
50
51
52
53
54
55
56
57
58
59
60

For TOC Use Only

